A Broad-Band Microwave Superconducting Thin-Film Transformer

DAVID P. McGINNIS AND JAMES B. BEYER, SENIOR MEMBER, IEEE

Abstract—**The design, construction, and testing of a broad-band superconducting transformer based on a Dolph–Chebyshev distribution is described. The transformer is completely compatible with thin-film circuit topologies and allows access to 50 Ω coaxial launchers. The transformer is a taper that utilizes only one side of the substrate and features a coplanar waveguide to microstrip transition without the use of via holes. The taper provides a characteristic impedance transformation from 50 Ω to 2 Ω over a frequency range from 5 to 15 GHz. The taper provides a much larger bandwidth than a linear taper with the same length and impedance transformation.**

I. Introduction

BECAUSE MOST superconducting devices are fabricated with thin films, the input and output impedance levels of many of these devices are usually very low [1]–[4]. Insertion loss associated with a large impedance mismatch restricts the use of these devices in 50 Ω microwave systems. This paper presents the design approach, fabrication procedure, and test results of a broad-band superconducting impedance transformer. The transformer is completely compatible with thin-film circuits and allows access to 50 Ω coaxial launchers. The transformer is a taper that utilizes only one side of the substrate and features a coplanar waveguide to microstrip transition without the use of via holes.

II. Theory and Design Procedure

Because of its broad-band frequency characteristics, the impedance transformer that will be considered in this paper is a transmission line taper. The taper consists of a transmission line in which the characteristic impedance is smoothly tapered from one end of the line to the other. The taper can be thought of as a high-pass filter. The low-end cutoff frequency (f_0) occurs when the taper is half a wavelength long.

It will be assumed that a single forward propagating mode and a single reverse propagating mode exist in the taper. The characteristic impedance profile of the taper as a function of length is chosen so that the coupling between these two modes is minimized. One such profile that does minimize the coupling is the Dolph–Chebyshev distribution [5]. The characteristic impedance as a function of position (x) for this distribution is given as

$$Z(\xi) = Z_1 \exp\left[\ln\left(\frac{Z_2}{Z_1}\right)\int_{-\beta_0 L}^{\xi} K(\xi')\,d\xi'\right] \tag{1}$$

where Z_1 and Z_2 are the characteristic impedances at the beginning and the end of the taper, respectively. Also,

$$x = (\xi + \beta_0 L)/2\beta_0 \tag{2}$$

and

$$\beta_0 = \frac{2\pi f_0}{v_{\text{ph}}} \tag{3}$$

where L is the length of the taper, v_{ph} is the phase velocity of the propagating modes in the taper, and f_0 is the desired low-end cutoff frequency of the taper. The kernel of the integral in (1) can be expanded in a Fourier series. To simplify the taper design, we will include only the first term in the series. The coefficient of the first term can be determined from boundary conditions to be 0.25 [5]. The characteristic impedance as a function of position (x) then reduces to

$$Z = Z_1 \exp\left\{\frac{1}{2}\ln\left(\frac{Z_2}{Z_1}\right)\left[\sin\left(\pi\left(\frac{X}{L}-\frac{1}{2}\right)\right)+1\right]\right\}. \tag{4}$$

A plot of the characteristic impedance as a function of length for a taper with a length of 15 mm, an impedance transformation from 2 Ω to 50 Ω, a phase velocity of $0.4c$, and a cutoff frequency of 4 GHz is shown in Fig. 1.

The scheme shown in Fig. 2 can be used to demonstrate the performance of the taper of Fig. 1. The system consists of the taper, a section of 2 Ω transmission line, and a second taper from 2 Ω back to 50 Ω. The length of the 2 Ω section of transmission line is 15.7 mm. For demonstration purposes, the phase velocity throughout the circuit was assumed to be 40 percent of the velocity of light in vacuum. The forward scattering parameter (S_{21}) as a function of frequency for the scheme of Fig. 2 is shown in Fig. 3. Also shown in Fig. 3 is S_{21} as a function of frequency utilizing tapers in which the impedance profile varies linearly from 2 Ω to 50 Ω. The responses of the tapers were determined by segmenting the tapers into 100 two-port sections and using a microwave CAD program (TOUCHSTONE ver 1.4). As shown in Fig. 3, the bandpass char-

Manuscript received February 19, 1988; revised May 13, 1988. This work was supported by the Air Force Office of Scientific Research under Grant AFOSR-86-0025.

D. P. McGinnis was with the Department of Electrical and Computer Engineering, University of Wisconsin at Madison, Madison, WI. He is now with Fermilab, Batavia, IL 60510.

J. B. Beyer is with the Department of Electrical and Computer Engineering, University of Wisconsin at Madison, Madison, WI 53706-1691.

IEEE Log Number 8823258.

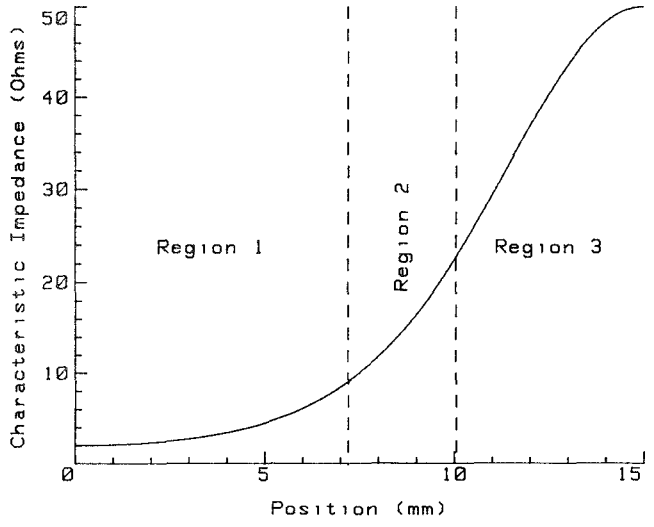

Fig. 1. Characteristic impedance of the taper as a function of length.

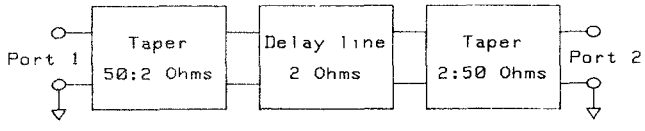

Fig. 2. Transmission line circuit incorporating the impedance taper.

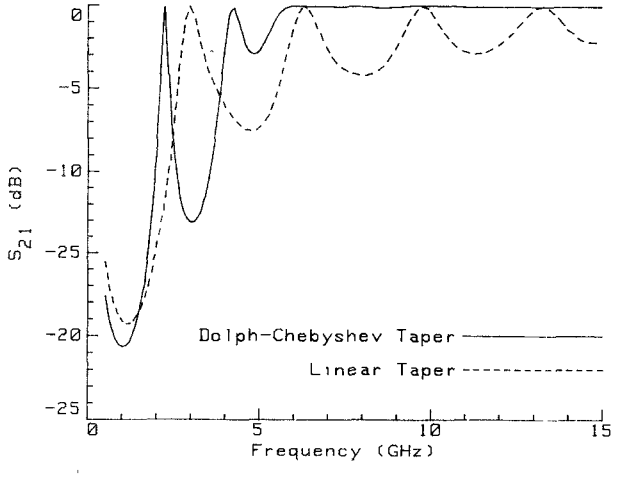

Fig. 3. The forward scattering parameter (S_{21}) as a function of frequency for a Dolph–Chebyshev taper and a linear taper.

acteristics of the taper described by (4) are much more desirable than those of the linear taper.

The taper in this study was also required to provide a geometrical transformation from a 50 Ω coaxial environment to a low-impedance microstrip topology. To perform this task, our thin-film taper itself consists of three sections. These sections are a low-impedance microstrip section (region 1, Fig. 1; 2–8 Ω), a transition region consisting of a microstrip–coplanar waveguide hybrid (region 2, Fig. 1; 8–23 Ω), and a high-impedance coplanar waveguide segment (region 3, Fig. 1; 23–50 Ω). The end of the high-impedance segment interfaces with a 50 Ω coaxial launcher. To eliminate the difficulties associated with fabricating via holes, it is desirable to keep the ground

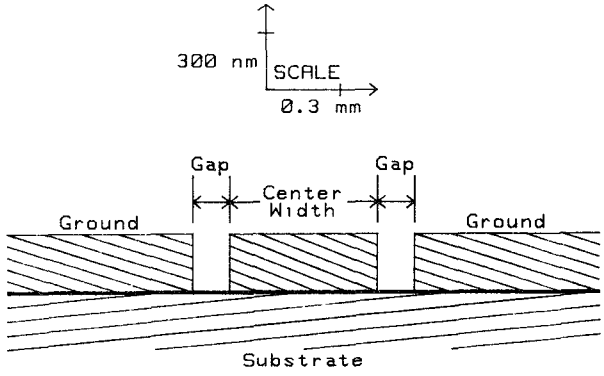

Fig. 4. Cross-sectional view of a coplanar waveguide.

plane and the circuit on the same side of the substrate. Thus, the high-impedance section of the taper was chosen to be coplanar waveguide.

The coplanar waveguide consists of a center thin-film strip surrounded by two ground planes on either side of the center conductor as shown in Fig. 4. The characteristic impedance of the coplanar waveguide is a complicated function of the width of the center conductor and the gap between the center strip and outer ground planes [6]. The values of the characteristic impedance and the phase velocity for the coplanar waveguide were determined using a microwave circuit CAD program (TOUCHSTONE). For a silicon substrate with a dielectric constant of 12, the reasonable range of characteristic impedances obtainable with the coplanar waveguide lies between 20 Ω and 100 Ω [7]. The phase velocity is approximately 42 percent of the velocity of light in vacuum, which correlates to an effective dielectric constant of 5.7. The loss associated with the silicon substrate is negligible because the semiconductor carriers are frozen out by cooling with liquid helium to a temperature of 4.2 K.

The first section of the taper is intended to interface with a low-impedance superconducting device. Coplanar waveguide could not be used to reach the desired range of low impedances. Superconducting microstrip was chosen instead because it can be fabricated to very low characteristic impedances and yet provide very small propagation losses. In the limit of very small characteristic impedance, the microstrip can be modeled by parallel-plate formulas.

Because the parallel plates are closely spaced, the complex surface impedance of the superconductors must be included in the expression for the characteristic impedance. The characteristic impedance of a parallel-plate transmission line is [8]

$$Z_0 = \frac{d}{W}\sqrt{\frac{\mu_0}{\epsilon_0 \epsilon_r}}\left[\frac{2\lambda + d}{d}\right]^{1/2} \tag{5}$$

where W is the width of the plates, d is the spacing between the plates, ϵ_r is the effective permittivity of the dielectric between the plates, and λ is the London penetration depth of the superconductors. The London penetration depth of thin-film niobium is approximately 100 nm.

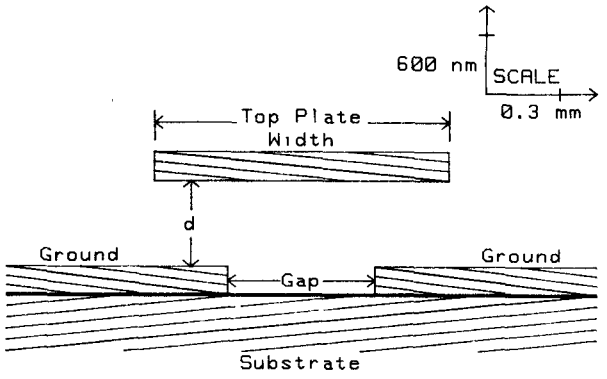

Fig. 5. Cross-sectional view of the parallel-plate transmission line with a split ground plane.

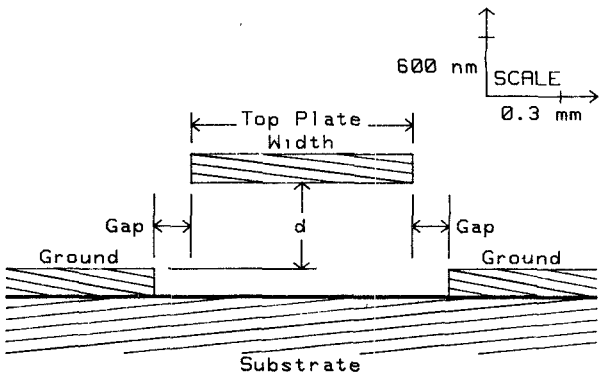

Fig. 6. Cross-sectional view of a modified coplanar waveguide.

The phase velocity in the parallel plate line is given as [8]

$$v_{\text{ph}} = \frac{1}{\sqrt{\mu_0 \epsilon_0 \epsilon_r}} \left[\frac{d}{2\lambda + d} \right]^{1/2}. \tag{6}$$

To keep the phase velocity in the parallel-plate transmission line in the same range as the phase velocity of the coplanar waveguide, silicon monoxide (SiO), which has a relative permittivity of approximately 6, was chosen for the dielectric between the parallel plates. Using (6) with a dielectric thickness of 1 μm, the phase velocity in the parallel-plate transmission line is 37 percent of the velocity of light in vacuum. Because the exact dielectric constant of the thin-film silicon monoxide is unknown due to variations in the dielectric thickness and composition as a result of using thin-film fabrication techniques, it will be assumed for simplicity of design that the phase velocity in the parallel-plate transmission line is the same as in the coplanar waveguide.

If a small gap in the ground plane under the center conductor of the parallel-plate section of transmission line can be introduced, then the characteristic impedance of the parallel-plate transmission line can be varied by changing the gap width of the ground plane as shown in Fig. 5. The split in the ground plane will reduce the capacitance and increase the inductance of the transmission line so that the characteristic impedance given by (5) can be modified as

$$Z_0 = \frac{d}{W - G} \sqrt{\frac{\mu_0}{\epsilon_0 \epsilon_r}} \left[\frac{2\lambda + d}{d} \right]^{1/2} \tag{7}$$

where W is the width of the top plate and G is the gap in the ground plane. This approximation should be valid until the dielectric thickness is greater than 5 percent of the width of the top plate minus the gap in the ground plane. Near this point, the parallel-plate approximations break down and fringing fields should be taken into account.

The parallel-plate section is a vertical structure which spans three planes (see Fig. 5). A true coplanar waveguide segment is located within one plane as shown in Fig. 4. However, to bridge this mismatch in geometry, the coplanar waveguide is fabricated in three planes as shown in Fig. 6. Because the film thicknesses are much smaller than the lateral dimensions, coplanar waveguide descriptions are still valid for describing this structure.

According to (5), the width of the top plate in the parallel-plate regime must narrow down to 80 μm if the characteristic impedance of 2 Ω is to be achieved. However, the width of the center conductor of coplanar waveguide should approach 550 μm if the coplanar waveguide is to match to a 50 Ω SMA coaxial launcher. It can be seen by comparing Fig. 5 with Fig. 6 that the top plate of the parallel-plate section and the center conductor of the coplanar waveguide region should be patterned on the same film layer. To compensate for the difference in width of the pattern, the top film is tapered using constant-radius curves. These curves are described by

$$W = W_p + 2R - 2\sqrt{R^2 - x^2} \tag{8}$$

for (x) less than $L/2$ (low-impedance region) and

$$W = W_c - 2R + 2\sqrt{R^2 - (x - L)^2} \tag{9}$$

for (x) greater than $L/2$ (high-impedance region), where

$$R = \frac{4L^2 + (W_c - W_p)^2}{8(W_c - W_p)} \tag{10}$$

and W_c is the width of the center conductor of the coplanar waveguide at $x = L$ and W_p is the width of the top plate of the parallel-plate transmission line at $x = 0$.

Once the impedance profile has been determined by (4) and the width of the top center film has been found by using (8)–(10), the gap in the ground plane or bottom film can be calculated. For impedances less than 8 Ω, the gap in the ground plane of the parallel-plate section was computed using (7). For impedances greater than 23 Ω, the gap in the ground plane for the coplanar waveguide segment was calculated using the TOUCHSTONE microwave circuit CAD program. Between 8 Ω and 23 Ω, the models for determining the characteristic impedance of the taper are not valid. Thus, the ground plane gap spacing was determined by interpolating between the two models using a curve of the form

$$X^2 + AXG + BG^2 + CX + DG = 0. \tag{11}$$

The constants A, B, C, and D were adjusted so that the

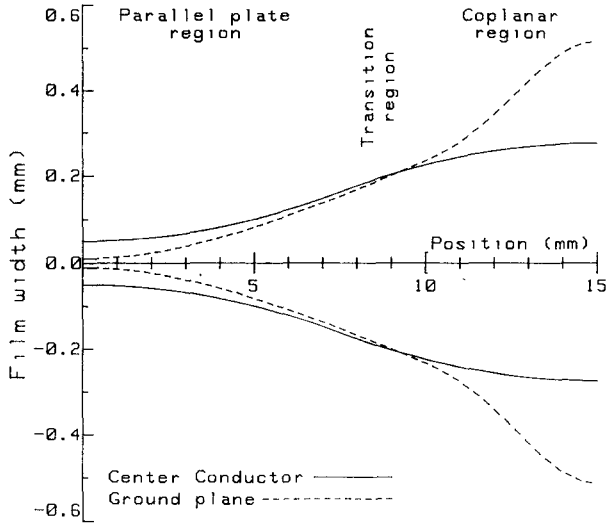

Fig. 7. The width of the center strip and gap in the ground plane as a function of position along the taper.

gap spacing and the first derivative of the gap spacing with respect to position along the taper were continuous at the 8 Ω and 23 Ω interfaces. The values of the constants are

$$A = -37.9 \qquad B = 300$$
$$C = -2870\ \mu\text{m} \qquad D = 65200\ \mu\text{m}.$$

A plot of the center conductor width and the ground plane gap as a function of position along the taper is shown in Fig. 7.

III. Results

The thin-film layout of the circuit shown in Fig. 2 is shown in Fig. 8. The substrate was 400 μm-thick single crystal silicon. The ground plane was fabricated with niobium deposited by a dc magnetron to a thickness of 300 nm. The ground plane was patterned by plasma etching. The dielectric layer was fashioned by evaporating SiO to a thickness of 1 μm. The dielectric layer was patterned with a photoresist lift-off technique. Finally the top film which formed the center conductor was fabricated with Nb deposited by a dc magnetron to a thickness of 300 nm. The layer was patterned with plasma etching.

The forward transmission scattering parameter, S_{21}, was measured from 100 MHz to 15 GHz using an HP-8510 network analyzer. The results are displayed in Fig. 9. The maximum level of S_{21} at −1.5 dB can be attributed to attenuation in the 1 m lengths of semirigid coaxial cable needed to connect the network analyzer with the cryogenic environment. The response shown in Fig. 9 compares favorably to the theoretical response shown in Fig. 3, with the exception of two dropouts in the frequency response of S_{21} near 4 and 8 GHz.

To explain the origin of these dropouts, a thin-film circuit was fabricated that replaced the 2 Ω section of transmission line with a single short circuit between the top conductors of both tapers and the ground plane. To ensure that the short circuit was a true short and that there was no coupling through the microstrip line, the length

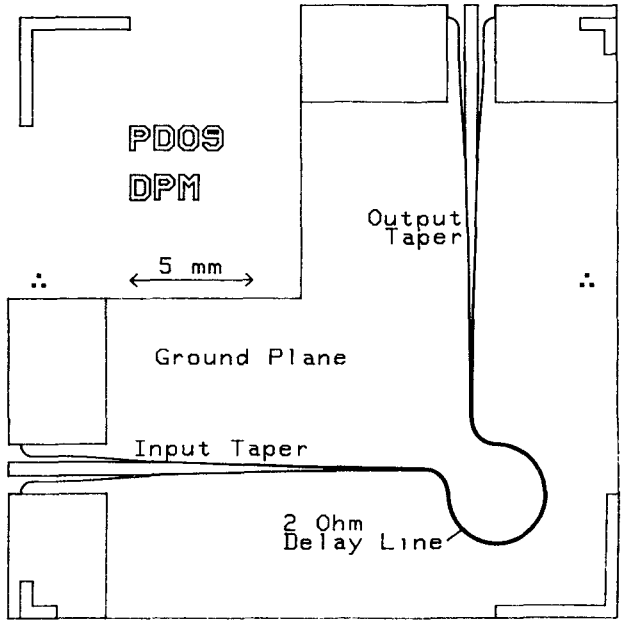

Fig. 8. A thin-film layout of the impedance taper circuit.

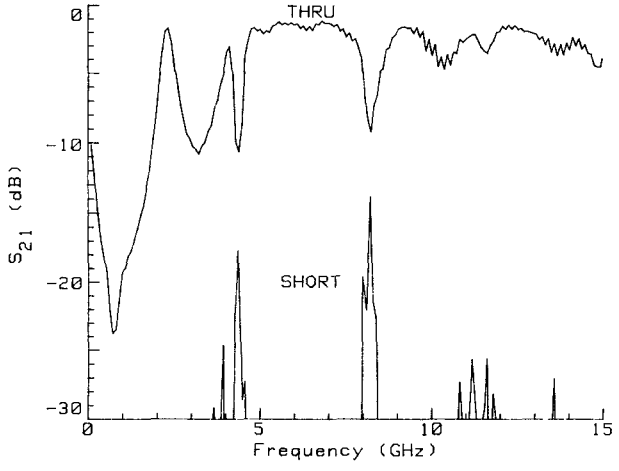

Fig. 9. Experimental results of S_{21} as a function of frequency for the Dolph–Chebyshev taper with a 2 Ω section of transmission line (top curve) and with a short circuit in place of the 2 Ω section of transmission line (bottom curve).

and the width of the short circuit were fabricated to be at least two orders of magnitude greater than the dielectric thickness and one order of magnitude greater than the width of the incoming sections of 2 Ω transmission line. Theoretically, there should be no transmission of signal between the input and output ports of the circuit. However, experimental data also shown in Fig. 9 reveal two peaks in the frequency response of S_{21} corresponding to the two dropouts. These peaks can be traced to resonances in the high-dielectric silicon substrate. The resonant modes in the substrate provide a path of crosstalk that adds out of phase with the signal propagating in the transmission line structure. Furthermore, S_{11} measurements taken during the through test did not show any significant reflection at the dropout frequencies, which supports the theory that energy is being coupled to substrate modes at these fre-

quencies. Thus, the dropouts in the response shown in Fig. 9 are not inherent in the taper design.

IV. Conclusions

This paper demonstrates a broad-band superconducting transformer based on a Dolph–Chebyshev distribution. The transformer is completely compatible with thin-film circuit topologies and allows access to 50 Ω coaxial launchers. The transformer is a taper that utilizes only one side of the substrate and features a coplanar waveguide to microstrip transition without the use of via holes. The taper provides a characteristic impedance transformation from 50 Ω to 2 Ω over a frequency range from 5 GHz to 15 GHz. The taper provides a much larger bandwidth than a linear taper with the same length and impedance transformation.

Acknowledgment

The authors wish to express their thanks to J. Nordman, G. Hohenwarter, and J. Martens for valuable discussions and assistance.

References

[1] K. K. Lihkarev, V. K. Semonov, O. V. Snigerev, and B. N. Todorov, "Josephson junction with lateral injection as a vortex transistor," *IEEE Trans. Magn.*, vol. MAG-15, no. 1, pp. 420–423, 1979.

[2] T. V. Rajeevakumar, "A Josephson vortex flow device," *Appl. Phys. Lett.*, vol. 39, pp. 439–441, 1981.

[3] B. J. Van Zeghbroeck, "Superconducting current injection transistor," *Appl. Phys. Lett.*, vol. 42, pp. 736–739, 1983.

[4] D. P. McGinnis, J. B. Beyer, and J. E. Nordman, "Distributed amplifiers using Josephson vortex flow transistors," *J. Appl. Phys.*, vol. 59, p. 3917, 1986.

[5] F. Sporleder and H. G. Unger, *Waveguide Tapers, Transitions, and Couplers*. London: Institution of Electrical Engineers, 1979, pp. 151–176.

[6] G. Ghione and C. Naldi, "Coplanar waveguides for MMIC applications," *IEEE Trans. Microwave Theory Tech.*, vol. MTT-35, pp. 260–267, Mar. 1987.

[7] R. E. Stegens and D. N. Alliss, "Coplanar microwave integrated circuits for integrated subsystems," *Microwave Syst. News Commun. Technol.*, vol. 87, p. 260, Oct. 1987.

[8] T. Van Duzer and C. W. Turner, *Principles of Superconductive Devices and Circuits*. New York: Elsevier North Holland, 1981, p. 134.

David P. McGinnis was born in Chicago, IL, on April 27, 1960. He received the B.S. degree in general engineering with a secondary field in physics in 1982 and the M.S. degree in physics in 1983, both from the University of Illinois at Urbana. He also received the M.S.E.E. and Ph.D. degrees in electrical engineering from the University of Wisconsin at Madison in 1984 and 1987, respectively. He is currently doing postdoctoral research at the University of Wisconsin at Madison in the area of superconducting microwave electronics.

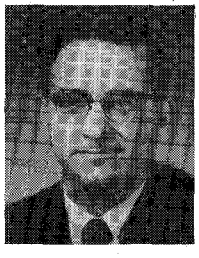

James B. Beyer (M'61–SM'79) received the B.S.E.E., M.S., and Ph.D. degrees from the University of Wisconsin, Madison, in 1957, 1959, and 1961 respectively.

From 1950 to 1954 he served in the U.S. Navy as a shipboard electronics technician. Upon resuming his studies in 1954 he held both research and teaching appointments at the University of Wisconsin. Since his appointment to the faculty in 1961 he has taught courses in the areas of electromagnetic fields, microwaves, antennas, and communications electronics. In 1968–69 he was a Fulbright Lecturer at the Technical University in Braunschweig, Germany. He is presently engaged in research on microwave integrated circuits and superconducting electronics.

Dr. Beyer is a member of Eta Kappa Nu and Sigma Xi.